High *p*-type doping of ZnBeSe using a modified delta-doping technique with N and Te

S. P. Guo,[a] W. Lin, X. Zhou, and M. C. Tamargo[b]
New York State Center for Advanced Technology on Photonic Materials and Applications, Center for Analysis of Structures and Interfaces (CASI), Department of Chemistry, City College-CUNY, New York, New York 10031

C. Tian, I. Kuskovsky, and G. F. Neumark
School of Mines and Department of Applied Physics, Columbia University, New York, New York 10027

(Received 12 February 2001; accepted for publication 17 May 2001)

High crystalline quality ZnBeSe epilayers were grown nearly lattice matched to GaAs (001) substrates by molecular beam epitaxy with a Be–Zn co-irradiation. A (1×2) reflection high energy electron diffraction pattern was observed after the Be–Zn co-irradiation of the GaAs (2×4) surface. A high *p*-type doping level of $1.5\times10^{18}\,\mathrm{cm}^{-3}$ was achieved for (N+Te) triple-delta doping (δ^3 doping) of ZnBeSe epilayers, whereby three adjacent δ layers of N and Te were deposited in each doping cycle. X-ray diffraction measurements reveal that (N+Te) δ^3-doped ZnBeSe samples with a Te concentration of about 0.5% remain of very high crystalline quality with an X-ray rocking curve linewidth of 51 arcsec. Low temperature photoluminescence measurements show some emission peaks related to Te_2 clusters and/or $Te_{n\geqslant 3}$ clusters. © *2001 American Institute of Physics.* [DOI: 10.1063/1.1384863]

I. INTRODUCTION

Blue-green laser diodes (LDs) are interesting because of their applications for high capacity storage and for full-color displays. The first ZnCdSe/(Zn,Mg)(S,Se)-based blue-green LD was demonstrated in 1991.[1,2] However, so far, the lifetime of such a LD is limited to ~500 h due to the degradation of the devices.[3,4] Considering the small lattice constant (5.139 Å) and the large band gap energy ($E_g>5$ eV), BeSe is a very good candidate to replace ZnS in the (Zn,Mg)(S,Se) alloys. One reason is that the epitaxial growth is much more controllable and reproducible when an alloy contains several metals and only a single nonmetal, rather than several nonmetals. Another reason is that beryllium chalcogenides have a high degree of covalent bonding compared to other wide gap II–VI semiconductors and are expected to have high bonding energies[5] and increased hardness,[6] which may increase the crystalline quality and material hardness, and, thus further improve the device lifetime.

The *p*-type doping is a prevalent difficult issue in wide band gap semiconductors. Using a discharge nitrogen plasma source one can dope ZnSe *p*-type to $\sim1\times10^{18}\,\mathrm{cm}^{-3}$ and ZnMgSSe with a $E_g\sim3$ eV to low $10^{17}\,\mathrm{cm}^{-3}$.[4,7,8] Such a doping level is not high enough to make good ohmic contacts for a laser structure. Delta doping (δ doping) has been proposed to reduce the complex-type compensating defects and to increase the *p*-type doping level.[9,10] However, the net acceptor concentration (n_a-n_d) is only $\sim1\times10^{18}\,\mathrm{cm}^{-3}$ for δ-doped ZnSe with N alone. Considering the high *p*-type doping ability in ZnTe, it is useful to introduce Te in ZnSe for *p*-type doping. A high *p*-type doping level of $7\times10^{18}\,\mathrm{cm}^{-3}$ has been reported by Jung *et al.*[11] using delta doping of a ZnSe/ZnTe:N superlattice, where full monolayers (ML) of highly N-doped ZnTe are separated by 10 ML of undoped ZnSe. This structure consists of ~9% ZnTe, resulting in ~0.7% lattice mismatch to ZnSe. Recently, using a modified (N+Te) δ-doping technique,[12] a similar *p*-type doping level (n_a-n_d) of $6\times10^{18}\,\mathrm{cm}^{-3}$ was achieved with an average Te content of only 2%–3%, corresponding to ~0.2% lattice mismatch to ZnSe.

So far, the highest reported *p*-type doping level in ZnBeSe or ZnBeMgSe is $\sim2\times10^{17}\,\mathrm{cm}^{-3}$.[13–15] The limited doping level may be due to the solubility limit or compensation mechanisms. In this article, we report the use of a modified (N+Te) δ-doping technique to enhance the *p*-type doping level in ZnBeSe. A (n_a-n_d) value of $1.5\times10^{18}\,\mathrm{cm}^{-3}$ was achieved for a (N+Te) triple-delta-doped (δ^3-doped) ZnBeSe sample with a low Te content of 0.5% and a narrow x-ray rocking curve with a linewidth of 51 arcsec.

II. EXPERIMENTS

All the samples were grown nearly lattice matched to (001) GaAs substrates in a Riber 2300 molecular beam epitaxy (MBE) system with a III–V chamber and a II–VI chamber connected by ultrahigh vacuum. Oxide desorption of the substrate was performed in the III–V chamber by heating to ~580 °C under an As flux, after which a 300 nm GaAs buffer layer was grown. The main shutter was closed at a substrate temperature (T_s) of 550 °C to maintain a (2×4) reflection high energy electron diffraction (RHEED) pattern. In order to avoid the formation of Ga_2Se_3 at the III–V/II–VI interface we performed Be–Zn co-irradiation before the growth of a 5 nm ZnSe buffer layer. Once the substrate with the GaAs buffer layer was transferred in vacuum to the II–VI chamber, the main shutter was opened immediately with the

[a]Current address: EMCORE Corporation, 394 Elizabeth Ave, Somerset, NJ 08873; electronic mail: shiping_guo@emcore.com
[b]Electronic mail: tamar@sci.ccny.cuny.edu

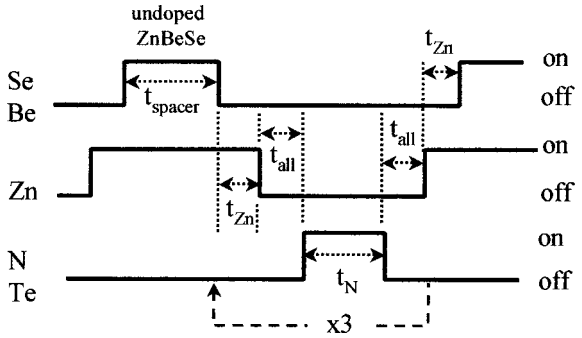

FIG. 1. Shutter control sequence of (N+Te) δ-doping and δ^3-doping techniques.

Zn and Be shutters open for 20 s. The RHEED pattern changes from (2×4) to (1×2) after the Be–Zn co-irradiation, a surface reconstruction not previously observed when Zn irradiation alone was used on the (001) GaAs (2×4) surface. The (1×2) RHEED pattern may be due to the formation of Be/Zn dimers on the GaAs surface.[13] Then the T_s was increased to 250 °C and the ZnSe buffer layer was grown. The RHEED pattern remains streaky and the surface reconstruction changes from (1×2) to (2×1) during the ZnSe growth. After this the T_s was increased to 270 °C and ZnBeSe epilayers were grown under Se-rich conditions. The RHEED pattern remains streaky (2×1) during the ZnBeSe growth. The *p*-type doping was achieved by employing an Oxford rf nitrogen plasma source. In order to make capacitance–voltage ($C-V$) measurements, p^+-GaAs substrates were used, and a *p*-type doped GaAs buffer layer was grown. For the bulk doping samples, a ~1 μm uniformly N-doped ZnBeSe layer was grown on the ZnSe:N buffer layer. For the modified (N+Te) δ-doping samples, a 0.5 μm uniformly N-doped layer was first grown followed by either ~0.4 μm (N+Te) δ-doped or δ^3-doped layer. Figure 1 shows the shutter control sequence used during the δ doping. An undoped ZnBeSe spacer was first grown for t_{spacer} seconds and then the Se and Be shutters were closed for t_{Zn} seconds to produce a Zn-terminated surface. Then, all shutters were closed for t_{all} seconds to desorb excess Zn from the surface, after which the N and Te shutters were open for t_N seconds to deposit N and Te atoms onto the Zn-terminated surface [(N+Te) co-doping]. After another growth interruption for t_{all} seconds, Zn was evaporated onto the N and Te containing surface for t_{Zn} seconds followed by opening the Se and Be shutters for the next ZnBeSe spacer growth. For the growth of the (N+Te) δ^3-doping samples, the shutter control sequence is similar to that of the (N+Te) δ-doping sequence except that the (N+Te) co-doping steps were repeated three consecutive times, as shown in Fig. 1, by the dashed arrow. The t_{spacer} was determined by the growth rate and the thickness of the spacer and $t_{Zn}=t_N=t_{all}=5$ s were chosen for the optimum results.[12]

The sample crystalline quality and the Be (or Te) content were assessed by double crystal x-ray diffraction (DCXRD) measurements using a Cu $K\alpha 1$ radiation. For etch pit density (EPD) measurements, a solution of methanol with 0.2% Br was used at room temperature (RT), which has been demonstrated to be suitable for ZnSe.[16] A solution of concentrated HCl (32%) was also used at 60 °C, which has been reported to be a suitable etchant for quaternary ZnMgSSe[17] and ZnBeMgSe.[18] Photoluminescence (PL) measurements were performed at 13 K using the 325 nm line of the He–Cd laser for excitation. $C-V$ measurements were carried out at RT using a gold contact with a diameter of 0.6 mm.

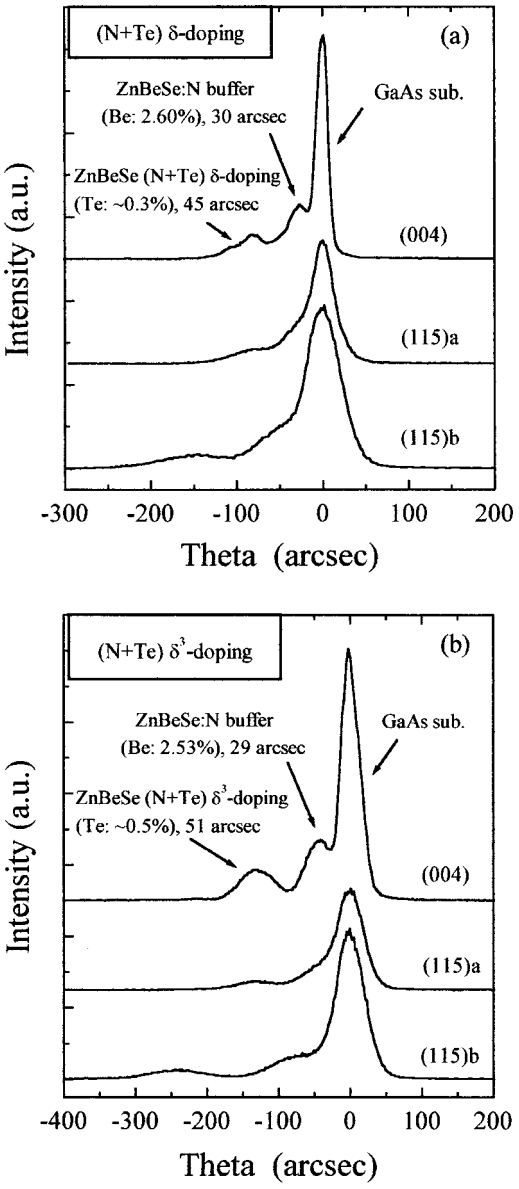

FIG. 2. The (004) symmetrical reflection and (115)*a* and *b* asymmetrical reflection DCXRD rocking curves for 100 periods of (N+Te) δ-doped (a) and δ^3-doped (b) ZnBeSe grown on a 0.5 μm uniformly N-doped ZnBeSe buffer layer.

III. RESULTS AND DISCUSSION

Figure 2 shows the (004) symmetrical reflection and the (115)*a* and *b* asymmetrical reflection DCXRD rocking curves for (N+Te) δ-doped (a) and δ^3-doped (b) ZnBeSe epilayers with 100 periods of 12 ML undoped ZnBeSe spacer layers separated by one (a) and three (b) (N+Te) containing layers, grown on a 0.5 μm uniformly N-doped ZnBeSe buffer layer. Three diffraction peaks can be clearly observed

TABLE I. XRD, EPD, and $C-V$ results of undoped, N-doped and (N+Te) δ-doped ZnBeSe epilayers.

	ZnBeSe	ZnBeSe:N	ZnBeSe:(N+Te)δ	ZnBeSe:(N+Te)δ^3
FWHM (arcsec)	23	30	45	51
Be content (%)	3.1	2.6	2.6	2.5
Te content (%)	0	0	0.3	0.5
EPD (cm^{-2})	4×10^4	1×10^5	6×10^5	5×10^5
n_a-n_d (cm^{-3})	···	2×10^{17}	3×10^{17}	1.5×10^{18}

for both cases. They are the diffraction peaks for the GaAs substrate, ZnBeSe:N buffer layer, and δ-doped or δ^3-doped ZnBeSe epilayers. The full width at half maximum (FWHM) of the (004) reflection x-ray rocking curves of the doped ZnBeSe epilayers is shown in Table I. For comparison, the FWHM for an undoped ZnBeSe epilayer (23 arcsec) was also listed in Table I.[13] The slight increase of FWHM (30 arcsec) for N-bulk doped ZnBeSe compared to the undoped layer may be related to the incorporation of nitrogen, which degrades the perfection of the lattice. The further increase of FWHM for the (N+Te) δ-doped and δ^3-doped ZnBeSe regions is due to the incorporation of Te atoms. Nevertheless, the FWHM for all these layers is 51 arcsec or less, indicating that all the epilayers still have very high crystalline quality. From the (115)a and b asymmetrical reflection DCXRD we can obtain the perpendicular and parallel lattice constant: a_1 and a_2 for both the bulk doped ZnBeSe:N buffer layer and the (N+Te) δ-doped or δ^3-doped layers. The bulk lattice constant then is calculated from the equation

$$a=a_1\{1-[2\nu/(1+\nu)][(a_1-a_2)/a_1]\}.$$

Here ν is the Poisson's Ratio (we use the value of ν for ZnSe of 0.28 for the ZnBeSe because of the small Be concentration). Assuming that Vegard's law is valid for ZnBeSe, the Be composition can be assessed from the lattice constant (shown in Table I). By further assuming that Vegard's law is also valid for ZnBeSe:(Te+N) and that the Be concentration is the same as that of the ZnBeSe:N buffer layer, the average Te content can be also estimated ($\sim$0.3% for the (N+Te) δ-doped layer and $\sim$0.5% for the δ^3-doped layer shown in Table I). In addition, EPD measurements were performed and the results are also shown in Table I. The EPD for an undoped ZnBeSe epilayer is very low ($4\times10^4\,cm^{-2}$), revealing an extremely high crystalline quality. It is a little higher for a N-bulk doped layer ($1\times10^5\,cm^{-2}$). The EPD for the (N+Te) δ-doped ($6\times10^5\,cm^{-2}$) or δ^3-doped ($5\times10^5\,cm^{-2}$) layers is one order of magnitude higher than that of the undoped layer. The high EPD in the (N+Te) δ-doped or δ^3-doped layers may be related to the incorporation of Te atoms, which introduce new defect nucleation centers. In addition, the long epitaxial growth process due to the very slow growth rate for the (N+Te) δ-doping ($\sim$0.3 μm/h) or δ^3-doping growth processes ($\sim$0.2 μm/h), may also increase the surface contamination and background doping level.

In order to study the electrical properties, both $C-V$ and electrochemical $C-V$ (ECV) measurements were performed at RT. From the slope of $1/C^2$ vs V a net acceptor concentration (n_a-n_d) can be calculated and the results are shown in Table I. The n_a-n_d is $\sim2\times10^{17}\,cm^{-3}$ for the N-bulk doped ZnBeSe epilayers, which is comparable to the highest reported value.[13,14] However, it is not high enough for electron injection devices, such as lasers, which carry a very high current. Using the modified (N+Te) δ-doping technique, the n_a-n_d was only slightly increased for the (N+Te) δ-doped ZnBeSe epilayers ($\sim3\times10^{17}\,cm^{-3}$), but it was dramatically increased to $1.5\times10^{18}\,cm^{-3}$ for the (N+Te) δ^3-doped ZnBeSe samples. The great enhancement of the p-type doping level in the (N+Te) δ^3-doped ZnBeSe samples is believed to be related to the effective isolation of N atoms from Se atoms. This may reduce the formation of compensation centers or it may also be due to the increase of the Te content, which enhances the solubility of N atoms and decreases the N activation energy. A large enhancement of p-type doping in ZnSe was reported using the same modified (N+Te) δ-doping technique,[12] where a n_a-n_d is $6\times10^{18}\,cm^{-3}$ was achieved and a nearly ohmic behavior was observed for (N+Te) δ^3-doped ZnSe epilayers with an average Te content of 2%–3%. This suggests that the modified (N+Te) δ-doping technique may have general application for p-type doping, especially for wide band gap semiconductors in which a high p-type doping level is usually difficult to achieve. It should be noted that by increasing the Be concentration one can put more Te in the δ-doped region for the ZnBeSe case and keep the lattice constant still nearly lattice matched to GaAs since the lattice constant of GaAs is between that of BeSe and of ZnTe. This may make it possible to achieve a high band gap with a reasonable p-type doping level as well as lattice matching.

Figure 3 shows the PL spectra of undoped (a), N-bulk doped (b), (N+Te) δ-doped (c), and (N+Te) δ^3-doped (d) ZnBeSe epilayers at 11 K. The undoped sample [spectrum (a)] is characterized by very sharp near band-edge emission and small peaks at the lower energy side. The dominant peak, at 2.856 eV, is attributed to a deep bound excitonic recombination[19] and it has isoelectronic origin.[20] The peaks at low energy are various (LO and TO) phonon replicas of the main peak.[19] In the N-bulk doped sample [spectrum (b)], there is a small band-edge peak at 2.844 eV, and a ''main'' peak at 2.774 eV with shoulders at 2.746 and 2.709 eV. The peak at 2.774 eV was assigned to donor–acceptor-pair (DAP) emission related to shallow impurities, including substitutional N.[15,19] The dominant contribution to the shoulders comes from the phonon replicas of the main peak.

The PL spectrum observed from the (N+Te) δ-doped ZnBeSe sample [spectrum (c)] is quite similar to that observed from the N-bulk doped sample. The only difference is

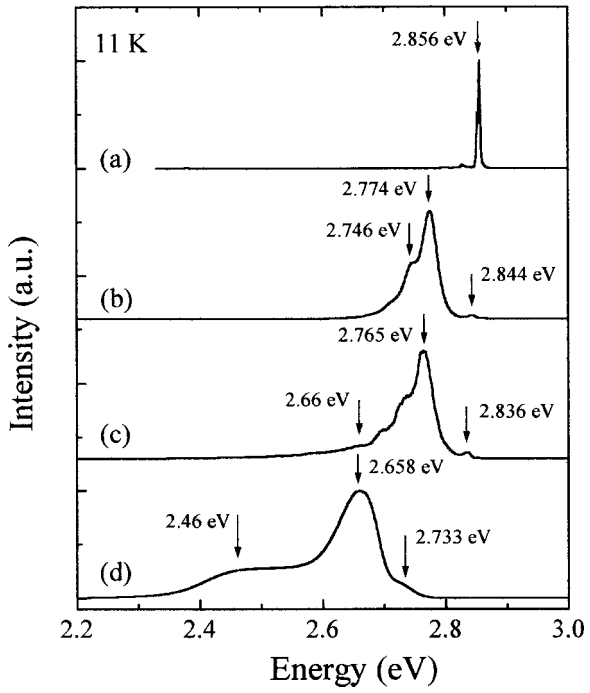

FIG. 3. PL spectra of undoped (a), N-bulk doped (b), (N+Te) δ-doped (c) and δ^3-doped (d) ZnBeSe epilayers at 11 K.

an appearance of a broad peak on the low energy side near 2.66 eV. This peak was previously attributed to excitons bound to Te complexes (Te_2 clusters and/or pairs) (Ref. 21 and references therein). It is interesting that while the concentration of Be is the same in both samples, the change in the energy of the band-edge PL emission is expected to come from the change in the band gap due to the presence of Te in the (N+Te) δ-doped sample. In fact, it has been reported that 0.3% of Te would result in reduction of the band gap by 6–8 meV,[22–24] which is consistent with the result observed here (8 meV).

The PL spectrum for the (N+Te) δ^3-doped ZnBeSe sample [spectrum (d)] is rather different. The dominant peak is at 2.658 eV (Te_2 complexes), while the band-edge peak has practically disappeared. Furthermore, the broad peak at around 2.46 eV is attributed to $Te_{n\geqslant 3}$ clusters.[21] The strong Te_2 cluster emission is consistent with the increase of Te content, which results in a higher concentration of Te_2 centers. The appearance of $Te_{n\geqslant 3}$ clusters in the (N+Te) δ^3-doped ZnBeSe sample comes from the higher amount of Te due to the presence of three adjacent Te containing layers in the δ^3-doped region. Detailed analysis of the PL results will be published elsewhere. The effective enhancement of the doping even with very small amounts of Te and the presence of $Te_{n\geqslant 3}$ clusters leads us to propose that submonolayer islands of ZnTe may be forming during the δ-doping process, with the N acceptors preferentially incorporated in these islands. The formation of nanoscale islands of similar materials, such as CdSe on ZnSe, has been previously reported.[25]

IV. CONCLUSIONS

In summary, high crystalline quality ZnBeSe epilayers were grown nearly lattice matched to GaAs (001) substrates by MBE using Be–Zn co-irradiation. A (1×2) RHEED pattern was observed after the Be–Zn co-irradiation of the GaAs (2×4) surface, suggesting the formation of Be/Zn dimers on the GaAs surface. Undoped ZnBeSe epilayers have a very narrow FWHM of the x-ray rocking curve of 23 arcsec with EPD as low as $4\times10^4\,cm^{-2}$. The FWHM was increased slightly, to 30 arcsec, for N-bulk doped epilayers, 45 arcsec for (N+Te) δ-doped epilayers and 51 arcsec for δ^3-doped epilayers, due to the incorporation of N and/or Te atoms. The Be and Te concentrations were estimated from the (115)*a* and *b* asymmetrical reflection DCXRD measurements. The Te content is ~0.3% for the (N+Te) δ-doped ZnBeSe and ~0.5% for the (N+Te) δ^3-doped ZnBeSe. The value of n_a-n_d is $2\times10^{17}\,cm^{-3}$ for the N-bulk doped ZnBeSe epilayers. It increases slightly for the (N+Te) δ-doping case, while it increases dramatically to $1.5\times10^{18}\,cm^{-3}$ for the (N+Te) δ^3-doping case. Low temperature PL measurements show emission peaks related to Te_2 and/or $Te_{n\geqslant 3}$ clusters.

ACKNOWLEDGMENT

The authors acknowledge the support of the National Science Foundation under Grant No. DMR9805760.

[1] M. A. Haase, J. Qiu, J. M. dePuydt, and H. Cheng, Appl. Phys. Lett. **59**, 1272 (1991).
[2] H. Heon, J. Ding, W. Patterson, A. V. Nurmikko, W. Xie, D. C. Grillo, M. Kobayashi, and R. L. Gunshor, Appl. Phys. Lett. **59**, 3619 (1991).
[3] L. L. Chao, G. S. Cargill III, C. Kothandaraman, T. Marshall, E. Snoeks, M. Buijs, K. Haberern, J. Petruzzello, G. M. Haugen, and K. K. Law, Appl. Phys. Lett. **70**, 535 (1997).
[4] S. Itoh, K. Nakano, and Ishibashi, J. Cryst. Growth **214/215**, 1029 (2000).
[5] F. Fischer, Th. Litz, H. J. Lugauer, U. Zehnder, Th. Gerhard, W. Ossau, A. Waag, and G. Landwehr, J. Cryst. Growth **175/176**, 619 (1997).
[6] A. Waag, F. Fischer, H. J. Lugauer, Th. Litz, T. Gerhard, J. Nürnberger, U. Lunz, U. Zehnder, W. Ossau, G. Landwehr, B. Roos, and H. Richter, Mater. Sci. Eng., B **B43**, 65 (1997).
[7] P. M. Mensz, S. Herko, K. W. Haberern, J. Gaines, and C. Ponzoni, Appl. Phys. Lett. **63**, 2800 (1993).
[8] D. C. Grillo, Appl. Phys. Lett. **63**, 2723 (1993).
[9] Z. Zhu, G. D. Brownlin, G. Horsburgh, P. J. Thompson, S. Y. Wang, K. A. Prior, and B. C. Cavenett, Appl. Phys. Lett. **67**, 2167 (1995).
[10] J. L. De Miguel, S. M. Shibli, M. C. Tamargo, and B. J. Skromme, Appl. Phys. Lett. **53**, 2065 (1988).
[11] H. D. Jung, C. D. Song, S. Q. Wang, K. Arai, Y. H. Wu, Z. Zhu, and T. Yao, Appl. Phys. Lett. **70**, 1143 (1997).
[12] W. Lin, S. P. Guo, M. C. Tamargo, I. Kuskovsky, C. Tian, and G. F. Neumark, Appl. Phys. Lett. **76**, 2205 (2000).
[13] S. P. Guo, Y. Luo, W. Lin, O. Maksimov, M. C. Tamargo, I. Kuskovsky, C. Tian, and G. F. Neumark, J. Cryst. Growth **208**, 205 (2000).
[14] H. J. Lugauer, Th. Litz, F. Fischer, A. Waag, T. Gerhard, U. Zehnder, W. Ossau, and G. Landwehr, J. Cryst. Growth **175/176**, 619 (1997).
[15] V. Bousquet, E. Tournié, M. Laügt, P. Vennéguès, and J. P. Faurie, Appl. Phys. Lett. **70**, 3564 (1997).
[16] A. Kamata and H. Mitsuhashi, J. Cryst. Growth **142**, 31 (1994).
[17] M. Shiraishi, S. Tomiya, S. Tanigachi, K. Nakano, A. Ishibashi, and M. Ikeda, Phys. Status Solidi A **152**, 377 (1995).
[18] F. Fischer, M. Keller, T. Gerhard, T. Behr, T. Litz, H. J. Lugauer, M. Keim, G. Reuscher, T. Baron, A. Waag, and G. Landwehr, J. Appl. Phys. **84**, 1650 (1998).
[19] I. Kuskovsky, C. Tian, C. Sudbrack, G. F. Neumark, S. P. Guo, and M. C. Tamargo, J. Cryst. Growth **214/215**, 1058 (2000).

[20] B. S. Kim, I. Kuskovsky, C. Tian, I. P. Herman, G. F. Neumark, S. P. Guo, and M. C. Tamargo, Appl. Phys. Lett. **78**, 4151 (2000).
[21] I. Kuskovsky, C. Tian, G. F. Neumark, J. E. Spanier, I. P. Herman, W. C. Lin, S. P. Guo, and M. C. Tamargo, Phys. Rev. B **63**, 155205 (2001).
[22] A. Yu. Naumov, S. A. Permogorov, A. N. Reznitskii, V. Ya. Zhulai, V. A. Novozhilov, and G. T. Petrovskii, Sov. Phys. Solid State **29**, 215 (1987).
[23] M. J. S. P. Brasil, R. E. Nahory, F. S. Turco-Sandroff, H. L. Gilchrist, and R. J. Martin, Appl. Phys. Lett. **58**, 2509 (1991).
[24] C. S. Yang, D. Y. Hong, C. Y. Lin, W. C. Chou, C. S. Ro, W. Y. Uen, W. H. Lan, and S. L. Tu, J. Appl. Phys. **83**, 2555 (1998).
[25] V. Ivanov, A. A. Toporov, T. V. Shubina, S. V. Sorokin, A. V. Lebedev, I. V. Sedova, P. S. Kop'ev, G. R. Pozina, J. P. Bergman, and B. Monemar, J. Appl. Phys. **83**, 3168 (1998).